Amplitude and phase filters for mitigation of defocus and third-order aberrations

Samir Mezouari, Gonzalo Muyo, Andrew R Harvey
Dept. of Computing and Electrical Engineering, Heriot-Watt University, Edinburgh, EH14 4AS, Scotland, United Kingdom

ABSTRACT
This paper gives a review on the design and use of both amplitude filters and phase filters to achieve a large focal depth in incoherent imaging systems. Traditional optical system design enhances the resolution of incoherent imaging systems by optical-only manipulations or some type of post-processing of an image that has been already recorded. A brief introduction to recent techniques to increase the depth of field by use of hybrid optical/digital imaging system is reported and its performance is compared with a conventional optical system. This technique, commonly named wavefront coding, employs an aspherical pupil plane element to encode the incident wavefront in such a way that the image recorded by the detector can be accurately restored over a large range of defocus. As reported in earlier work, this approach alleviates the effects of defocus and its related aberrations whilst maintaining diffraction-limited resolution. We explore the control of third order aberrations (spherical aberration, coma, astigmatism, and Petzval field curvature) through wavefront coding. This method offers the potential to implement diffraction-limited imaging systems using simple and low-cost lenses. Although these performances are associated with reductions in signal-to-noise ratio of the displayed image, the jointly optimised optical/digital hybrid imaging system can meet some specific requirements that are impossible to achieve with a traditional approach.

Keywords: Apodizer, depth of field, pupil plane, wavefront coding, defocus, spherical and third order aberration.

1. INTRODUCTION
In recent years, several approaches have been developed to design optical components that alleviate optical aberrations: coma, spherical aberration, astigmatism, field curvature, and chromatic aberration. These deviations are inherent to optical systems employing spherical surfaces though defects in manufacturing or alignment as well as the working environment can cause additional aberration such as defocus or thermal aberrations. Control of aberrations is mostly achieved by employing either amplitude filters or phase filters, but not both amplitude and phase simultaneously. Amplitude filters modify the light transmission to reduce the effect of aberrations of optical systems.[1-3] Various types of amplitude filters have been reported in the literature starting from the use of annular apertures where the effective pupil is considerably reduced (the pinhole camera is the extreme example), to those that employ the whole aperture using shaded filters.[4-9] Amplitude filters alleviate aberrations at the expense of the light transmitted by the optical system. For applications where high optical efficiency is essential, phase filters are traditionally employed. A phase plate, with a particular phase-delay function, modifies the transmitted wavefront to improve the quality of the point spread function (PSF).[10-15] More recently, Dowski et al.[16-18] used an aspherical phase filter to "encode" the transmitted wavefront and produce a PSF that is invariant to defocus and reduces the effect of third-order aberration. The recorded image can then be restored by digital processing. However, the enhancement of the performance achieved by this wavefront coding technique is accompanied by a reduction in the signal-to-noise ratio of the restored image. Furthermore, the non-radially symmetry of the phase plate shape means it is problematic to manufacture.

In this paper we to explore qualitatively the performance achieved by combining amplitude and phase functions into a single filter. A tradeoff process governs the optimisation of image quality by either of these filters and additional optimisation can be achieved by combining amplitude and phase filters. In the next two sections, we give a brief introduction to amplitude and phase filters and explore how they modify the variation of the Modulation Transfer Function (MTF). In sections 4 and 5 we explore the performance of a phase-only wavefront coding technique and we discuss and compare the use of different filters proposed in this work. In the last section, a brief physical insight into the Optical Transfer Function (OTF) for systems with wavefront coding is presented.

2. AMPLITUDE FILTERS

It is well established that a reduction in the effective size of the pupil induces an enhancement in the depth of focus of optical imaging systems.[1] Several methods have been used to design amplitude filters that produce high tolerance to aberrations where a particular attention is given to alleviate defocus and spherical aberrations. The evaluation of the Strehl ratio is the parameter mostly used to estimate the energy distribution along the optical axis and to assess the quality of the point spread function (PSF) close to the focal plane. Although various parameters can be used, such as the OTF, which illustrate the response of the optical system to various spatial frequencies, or more recently, the Wigner distribution function,[10] Strehl ratio is commonly used for its simplicity. This is particularly true when in it is possible to derive an analytical expression. Among the multitude of apodizers reported in the literature, we explore here the use of axially symmetric shaded filters that employ the whole pupil aperture and where the transparency of the amplitude filter varies across the pupil. As described by J. Ojeda-Castaneda et al.,[4-6] within an appropriate geometrical transformation mapping of the pupil coordinates it is possible to express the axial-intensity as a one dimension Fourier transform operation. By assuming a Gaussian distribution along the optical axis, the amplitude filter exhibits, therefore, a hyper-Gaussian transmission and the transmittance of the apodizer is given by

$$P(\rho) = e^{-\alpha\left((\rho/\rho_0)^2 - 1/2\right)^2} \tag{1}$$

where α is a positive real which controls the light throughput power as shown in Figure 1(a), ρ is the radial pupil coordinate, and ρ_0 represents the aperture radius. As illustrated in Figure 1(b), for small values of α the filter transmission across the whole pupil aperture is high. The transmittance falls quickly close the aperture edges as the values of α increase (α>20) and the filter acts like a smooth annular aperture of mean radius $\rho_0/\sqrt{2}$. According to Rayleigh's criterion, the Strehl ratio of 0.8 represents the lower limit to low aberration. Hence, Figure 2 displays the factor reduction of defocus W_{20} versus the parameter α. Within a finite interval of α, the tolerance to defocus is enhanced according to a linear regression, while the light throughput is reduced exponentially as the values of α increase. For example, when α=10 the light throughput is reduced severely (less than 0.2). To illustrate the performance of hyper-Gaussian apodizers, we calculate the MTF corresponding to several values of α with various magnitudes of defocus W_{20} and spherical aberrations W_{40}. According to Figure 3, it is clear that the performance achieved by hyper-Gaussian apodizers can be appreciated for α>10, at the expense of reduced optical efficiency. Furthermore, an attenuation of spatial frequencies just below the high-frequency cutoff causes some reduction in resolution. Therefore, the use of amplitude-only filters is suitable for applications where light throughput can be tolerated such as imaging with catadioptric optical systems, astronomical telescopes, or in scanning optical microscopes where annular apertures are employed.

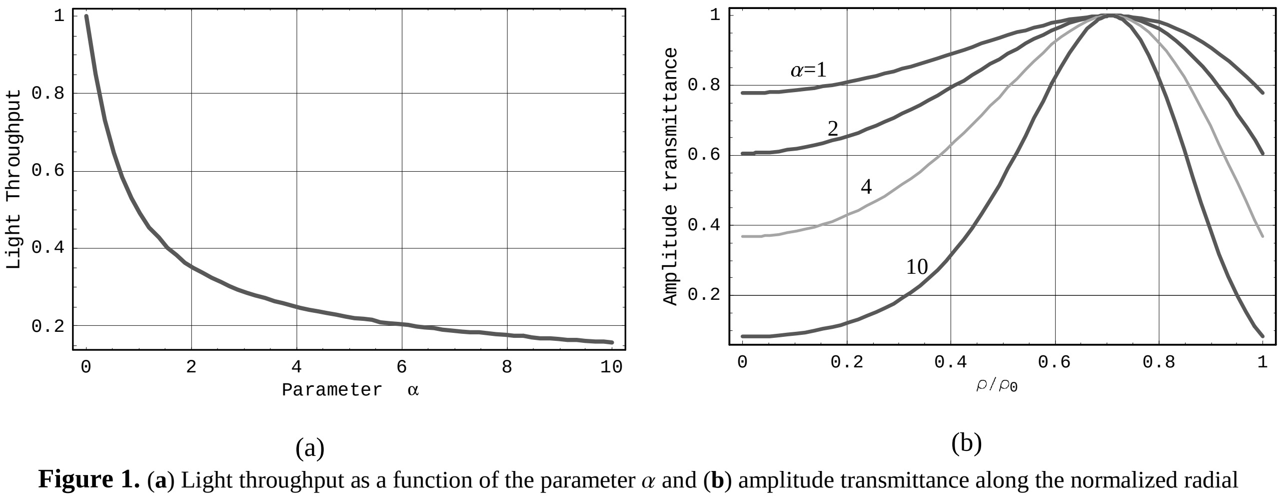

Figure 1. (**a**) Light throughput as a function of the parameter α and (**b**) amplitude transmittance along the normalized radial coordinate for different values of α.

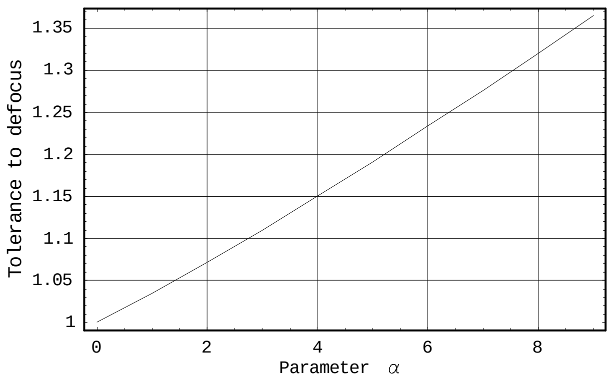

Figure 2. Reduction of the defocus parameter W_{20} versus the parameter α

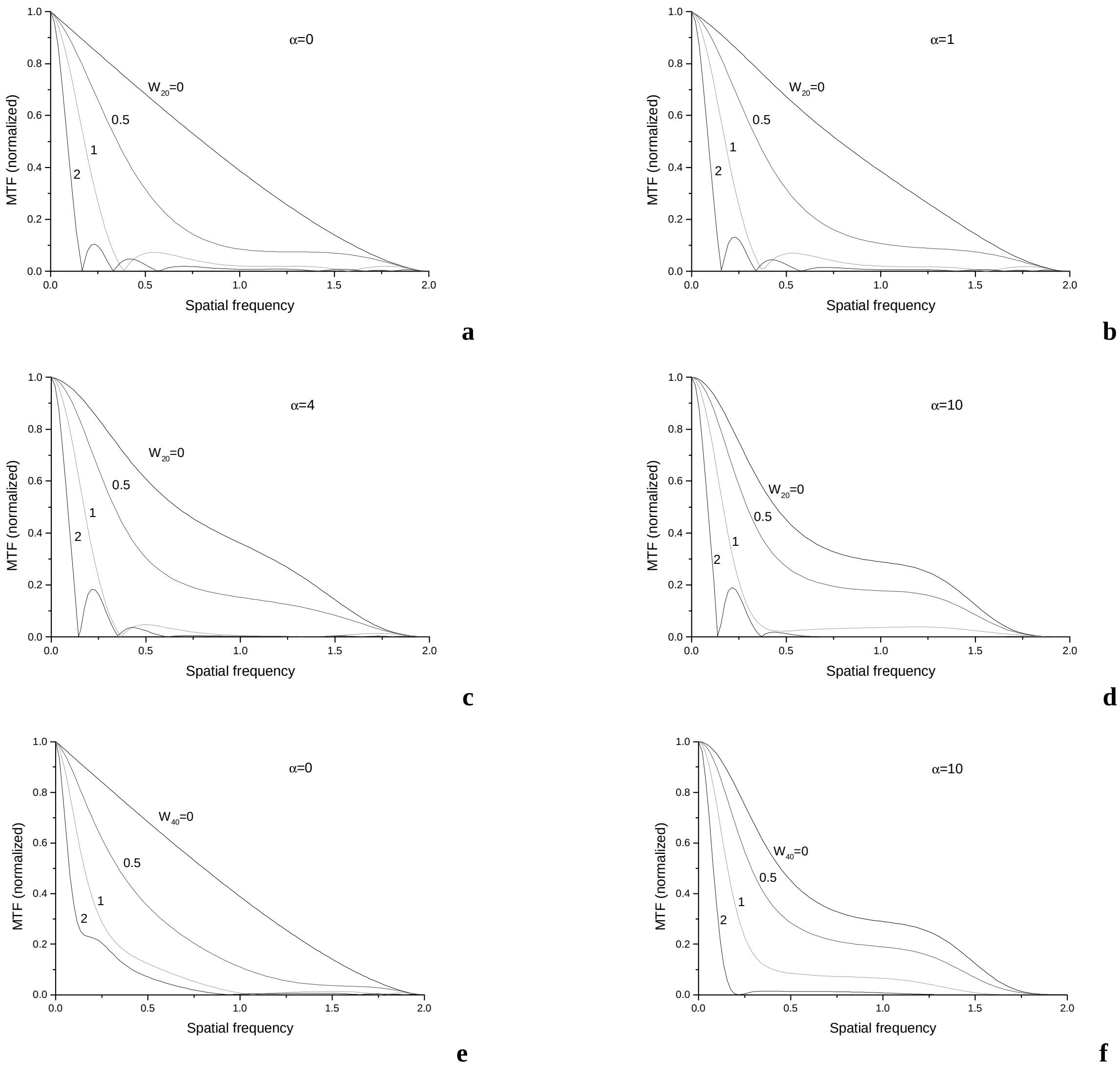

Figure 3. Computed MTFs (**a-d**) for four values of defocus W_{20}, and α= 0,1,4,10, and (**e-f**) for four values of spherical aberration W_{40} for α= 0,10

3. PHASE FILTERS

The phase filter is designed to introduce a phase modulation that reduces the effect of misfocus and spherical aberrations such that the aberrated PSF is a better approximation to an Airy disc. A similar analysis, as previous section, is applied to design phase filters that reduce optical aberrations inherent to imaging systems. We explore the performance of two phase-filters derived from the evaluation of Strehl ratio of axially symmetric systems. The choice of axially symmetric optical elements is dictated by the ease of manufacturing these elements, using, for example diamond machining. The expression of the phase-delay function of a quartic filter[11, 12] is given by

$$\theta(\rho) = 2\pi\hat{\alpha}\left((\rho/\rho_0)^2 - 1/2\right)^2 \qquad (2)$$

where $\hat{\alpha}$ is a real constant. As described in [**11**], when $\hat{\alpha}$ =0.75π the quartic filter achieves the largest depth of focus while the logarithmic filter is described by a phase-delay function [**12**] given by

$$\theta(\rho) = \bar{\alpha}\,(\rho/\rho_0)^4 + \bar{\beta}(\rho/\rho_0)^4 \log(\rho/\rho_0) \qquad (3)$$

where the parameters $\bar{\alpha}$ and $\bar{\beta}$ are real and chosen to control the optical performance. The variation of the point-spread function (PSF) in the presence of various aberrations for both, quartic and logarithmic filters can be found in our previous work.[13] A comparison between the MTFs obtained with optical systems suffering from defocus W_{20}, spherical aberration W_{40}, coma W_{31}, and astigmatism W_{22} is shown in Figure 4.

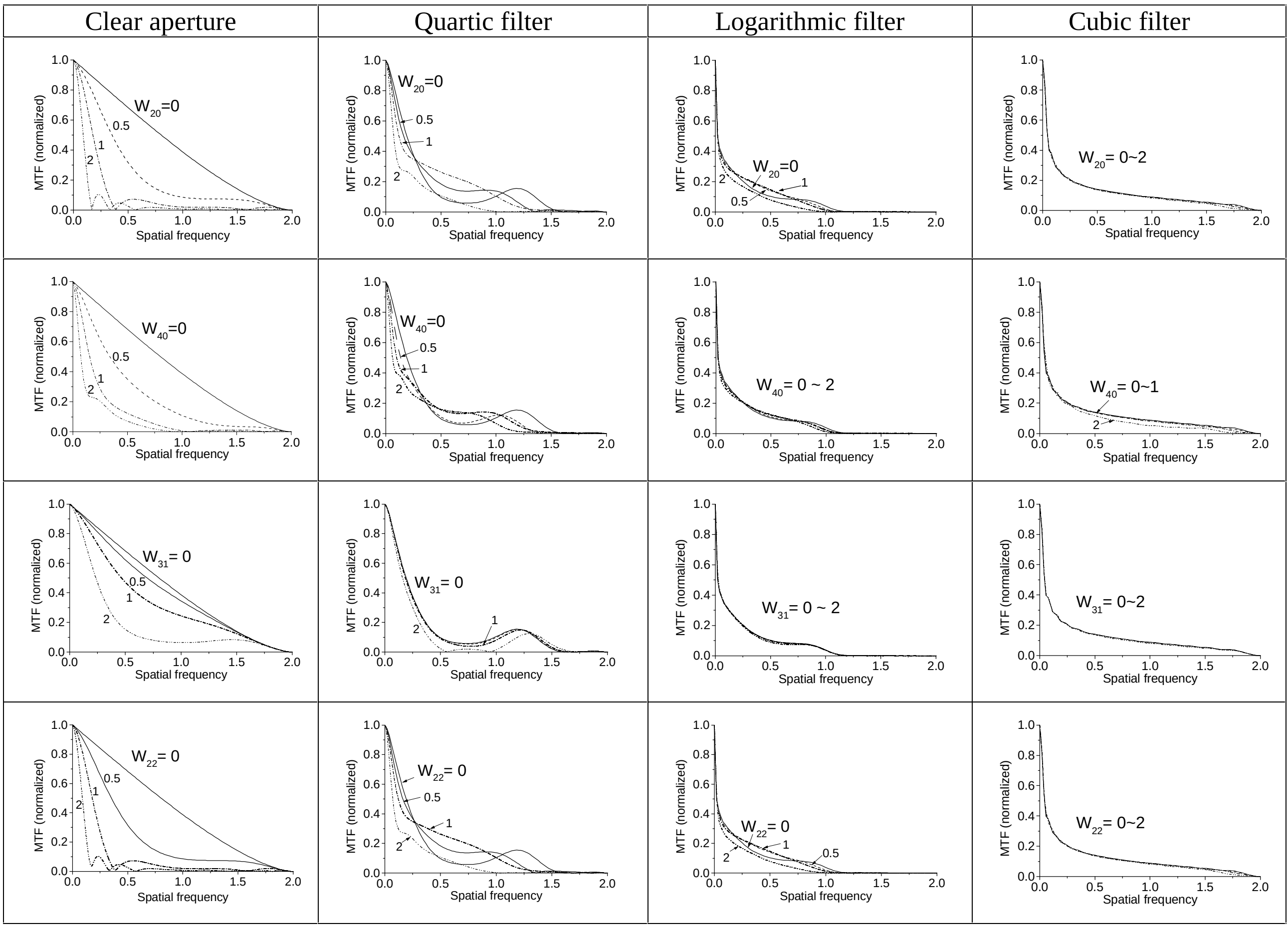

Figure 4. Computed MTFs obtained with optical systems suffering from defocus W_{20}, spherical aberration W_{40}, coma W_{31}, and astigmatism W_{22}.

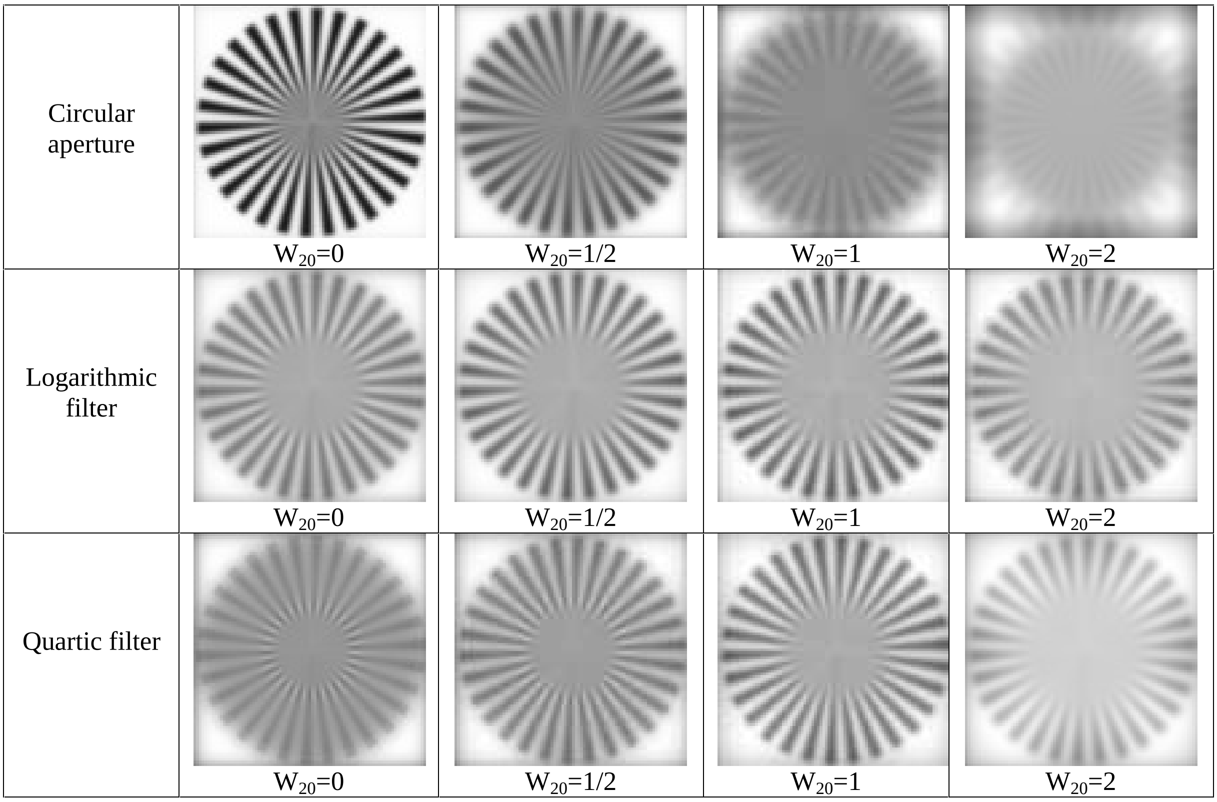

Figure 5. Computed images obtained with clear aperture, logarithmic filter, and quartic filter for various degrees of defocus

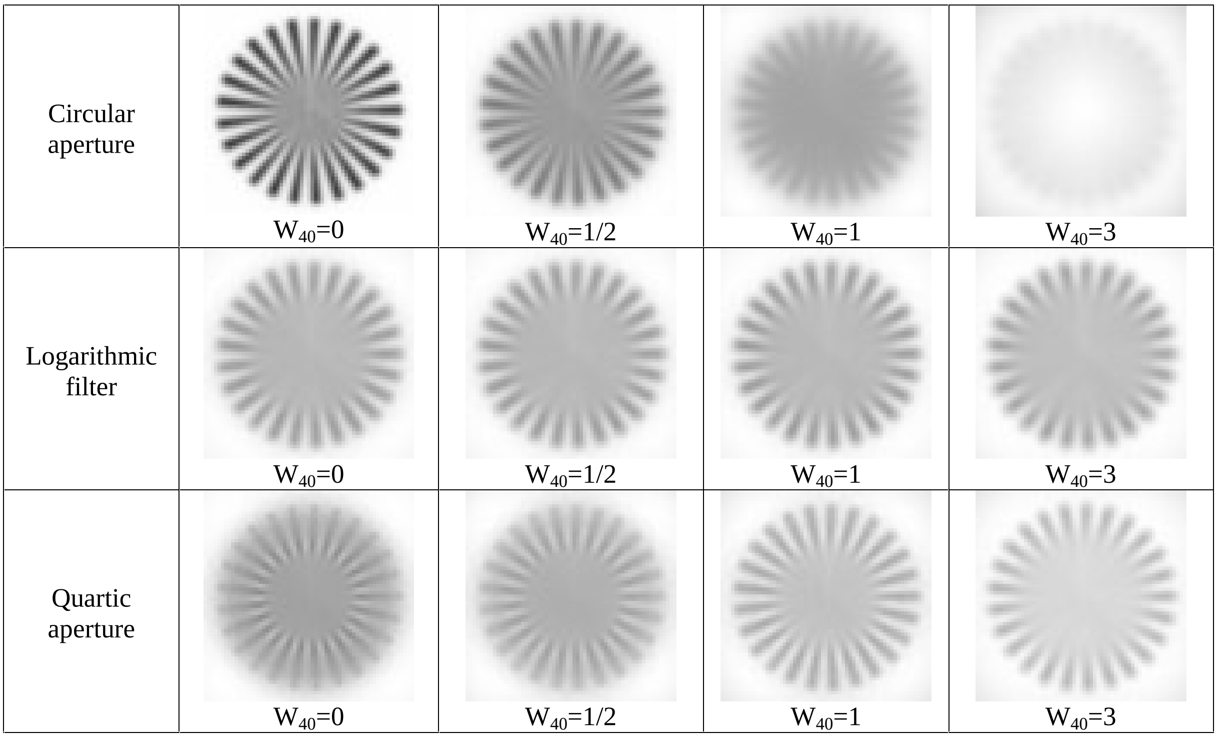

Figure 6. Computed images that suffer from spherical aberration obtained with clear aperture, logarithmic filter, and quartic filter.

It can be seen that the logarithmic phase filter achieves better tolerance to defocus aberration than the quartic filter. However, the loss in resolution at high spatial frequencies is more pronounced with the logarithmic filter (effective cutoff frequency is 65% of the diffraction-limited case) while the loss in resolution when a quartic phase filter is employed is less significant. The effect inherent in the use of both phase filters is to "lift" the relative response of the system at moderate spatial frequencies, which removes the presence of zeros in the MTF, and allows the deconvolution of the image without losing information within the bandpass. It is evident that the logarithmic filter displays high tolerance to spherical aberration while it reduces the resolution of the system. Similar observations as above are also valid for systems suffering from coma and astigmatism aberration. Therefore, phase filters offer better tolerance to primary aberrations, particularly the logarithmic phase filter, but at the expense of loss in resolution at high spatial frequencies and a reduction of the magnitude of the MTF overall frequencies. To appreciate the performance achieved by the logarithmic and quartic filter, we display in Figure 5 and Figure 6 the computed images that suffer respectively from defocus and spherical aberration.

4. WAVEFRONT CODING

Traditionally, aberrations are alleviated by introducing either optical modulation with amplitude or with phase filters, or by digitally processing the recorded image separately. Dowski et al proposed a new hybrid optical/digital configuration where an aspherical phase filter is used to produce an encoded image that is insensitive to defocus and some residual aberrations.[16] The encoded image can then be accurately restored computationally. The phase filter is designed from the evaluation of the optical transfer function of an incoherent imaging system by using the stationary phase approximation. The derived filters have rectangularly separable anti-symmetric phase shape and are given by

$$\theta(x, y) = \bar{\alpha}\left(x^3 + y^3\right) \quad (4)$$

where $\bar{\alpha}$ is a real variable that controls the peak-to-valley magnitude of the optical path difference introduced. Further details about the derivation of the cubic phase filter can be found in Ref.16. The performance achieved by the use of this wavefront coding is displayed through the calculated MTFs in the right column of figure 4 where $\bar{\alpha} = 4\pi^2$. Further to the discussion in the previous section, it is clear that the cubic phase filter offers a high tolerance to aberrations compared with the logarithmic and quartic filters. The MTFs displayed for the cubic filter, in Figure 4, are almost invariant to aberrations and contain no zeros. Although the magnitude of the MTF at high spatial frequencies is considerably reduced, the resolution is similar to the diffraction-limited performance. However, unlike the logarithmic and quartic filters, the image formed with the cubic phase filter is encoded and requires digital processing for display. This is a deconvolution process and therefore a loss in the signal-to-noise ratio (SNR) is expected[19] and in some cases can be considerable (when $\bar{\alpha} >> 1$) as shown in Figure 7. This noise amplification sets a serious limit to the system performance and depends substantially on the appropriate design of the phase filter. According to Figure 7, the noise amplification corresponding to $\bar{\alpha} = 4\pi^2$ is a factor of about 15 and this can result in a considerable reduction in image quality.

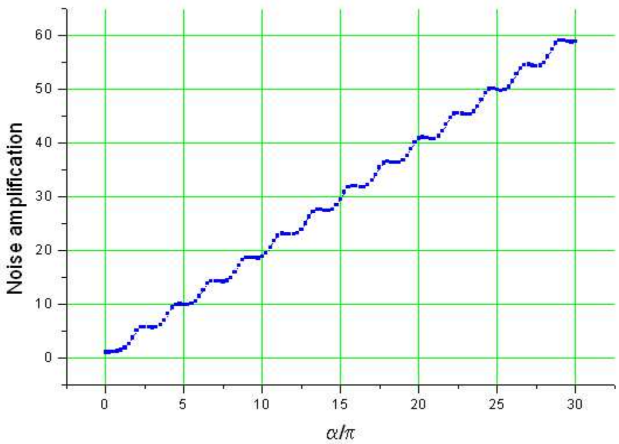

Figure 7. Variation of noise amplification as a function of peak-to-valley OPD of the cubic filter

This disadvantage is in addition, to the difficulties that arise in manufacturing an aspherical phase filter as the cubic mask, although in many cases an acceptable trade-off of noise amplification against aberration tolerance can be achieved. In the next section, we explore the use of complex amplitude *and* phase filters that could extend the system performance trade-off of noise amplification/light throughput/tolerance to aberrations.

5. COMPLEX AMPLITUDE AND PHASE FILTERS

So far, we have explored the use of phase-only or amplitude-only optical modulation to enhance system performance. We have shown that for amplitude filters an acceptable performance can be achieved by trading light throughput against tolerance to aberration, while for radially symmetric phase-only filters the alleviation of aberration is achieved by a reduction in resolution. Finally, the hybrid optical/digital wavefront coding technique offers a high tolerance to aberrations at the expense of a reduction in SNR of the final image. In this section, we explore the possibility of combining amplitude filters with wavefront coding to reduce the noise amplification effects at the cost of light throughput. Radially symmetric optical elements commonly called axicons and also holographic axilenses, that employ both amplitude and phase modulation have already been employed to produce a uniform optical intensity along the optical axis[20] and will not be discussed here.

In Figure 8(a), we present the MTF when a central circular obscuration is placed in front of the cubic phase filter. It can be seen that the use of an annular aperture provides some beneficial boost to the OTF at normalised spatial frequencies of about 1.5 at the expense of a reduction in MTF at normalised spatial frequencies of less than about 1.0. Although in some applications this might yield a small benefit, a further disadvantage is that the introduction of the annular aperture introduces much greater sensitivity to defocus as can be seen in Figure 8(b) and (c). It appears that although the use of a cubic phase mask alone or an annular aperture alone can beneficially reduce sensitivity to defocus, the use of a combined cubic phase mask and annular aperture is not beneficial.

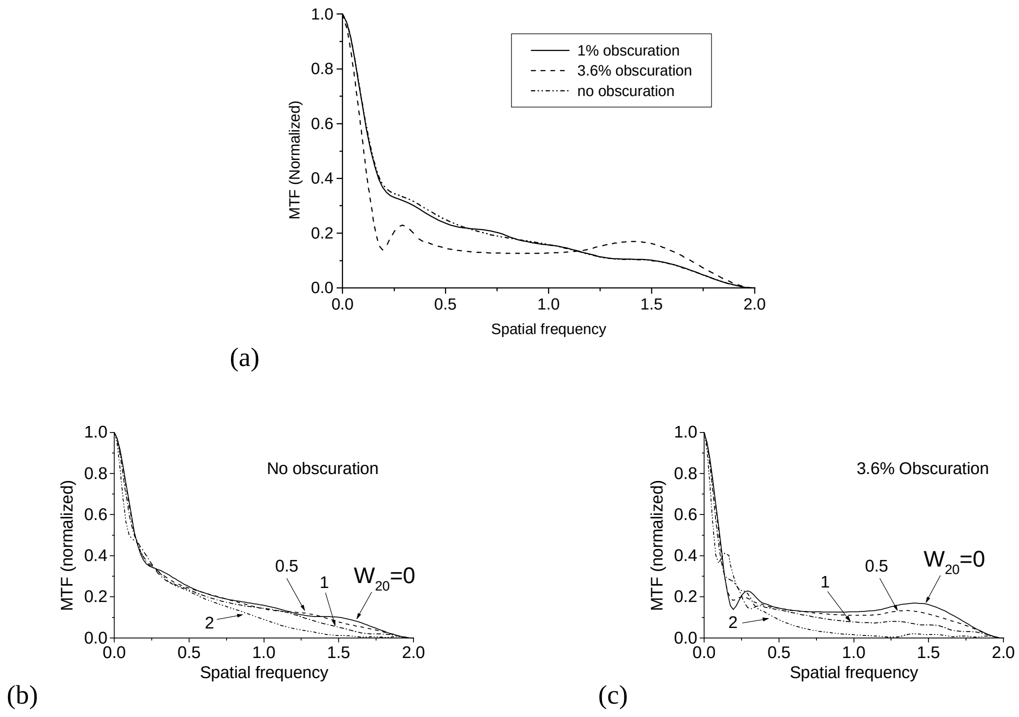

Figure 8. (a) In-focus MTF for a cubic phase mask and with a central aperture occupying 1% and 3.6% of the aperture area, (b) MTF of cubic phase mask with no obscuration and defocus of W_{20}=0, 0.5, 1 and 2 λ and (c) the same cubic phase mask with a 3.6% central obscuration and again with defocus of W_{20}=0, 0.5, 1 and 2 λ.

6. BRIEF PHYSICAL INSIGHT INTO THE WAVEFRONT CODED OTF

This last section gives a brief description of the physical insight into the Optical Transfer Function (OTF) of a system that is free from aberrations but suffers from defocus. We will assume a one–dimensional exit pupil to keep the mathematics simple. When the illumination of the object is incoherent, the OTF is determined by the normalized autocorrelation function of the generalized pupil function $\wp(x)$ of the system[21]:

$$H(f = \frac{\varepsilon}{\lambda z}) = \frac{\int_{-\infty}^{\infty} \wp\left(x + \frac{\varepsilon}{2}\right) \wp^{*}\left(x - \frac{\varepsilon}{2}\right) dx}{\int_{-\infty}^{\infty} \left|\wp(x)\right|^{2} \, dx} \tag{5}$$

where ε is the offset of the autocorrelation component dx, λ is the wavelength, z the distance from the centre of exit pupil to the image plane (radius of the Gaussian sphere), and f is the spatial frequency associated with ε. The numerator represents the region of overlap between the pupil function and itself but displaced by ε, one centred at $-\varepsilon/2$ and the other at $\varepsilon/2$, as shown in Fig. 9. The denominator is a normalising factor. When the separation ε is so large that the two pupils have no region in common, the value of the frequency transfer function is clearly zero; thus, spatial frequencies larger than a certain cut-off frequency are not transmitted by the system. In this particular case, for a one-dimensional aperture of width $2R$, the pupils will not overlap when $\varepsilon > 2R$,

$$f = \frac{\varepsilon}{\lambda z} > \frac{2R}{\lambda z} \tag{6}$$

When a fringe pattern of a particular frequency f is generated in the image plane, an interference effect takes place. This pattern can only be produced by the interference of light from two separate patches (or Young's pinholes) placed at the exit pupil of the system, with a separation ε between pinholes. Yet, for this particular spacing, many pairs of pinholes can be included in the pupil of the system. Each of them producing the same interference pattern of frequency f but shifted from the centred position. The number of ways a particular pair of Young's pinholes can be fit into the exit pupil is determined by the weighting factor applied by the system to that frequency component f.[22]

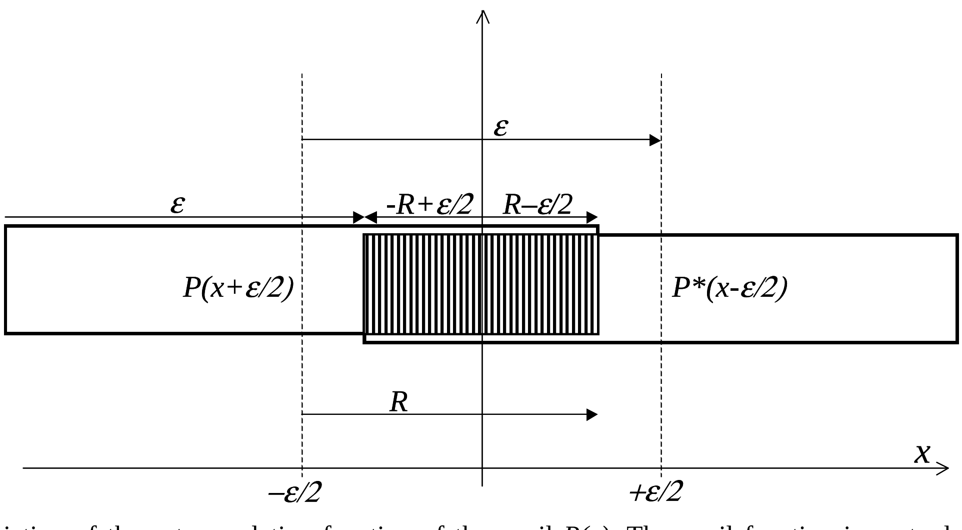

Figure 9. Depiction of the autocorrelation function of the pupil $P(x)$. The pupil function is centred at $-\varepsilon/2$ and its conjugate at $\varepsilon/2$. The area of overlap between the two pupils, with a particular spacing ε, is proportional to the modulus of the OTF for the corresponding spatial frequency f, where $f=\varepsilon/\lambda z$.

In terms of the OTF, this relative weigh for the frequency *f* is proportional to the area of overlap of two pupils separated by the corresponding spacing ε. Therefore, as the separation between pairs of Young's pinholes increases, generating higher spatial frequencies, there will be fewer ways in which these pinholes can be embraced by the pupil and as result the OTF will decrease, reaching the value zero at the cut-off frequency. At this particular frequency the separation between the pair of pinholes will be larger than the pupil, and consequently that frequency will not be transmitted by the system, as the pinholes cannot be fit in the pupil.
Let's consider now the autocorrelation function when applied to aberrated optical system. As mentioned before, each infinitesimal element dx in the area of overlap represent the contribution to the OTF of a single pair of Young's pinholes placed in a certain position x at the exit pupil and separated by a distance ε. This contribution will be represented by a phasor, which describes a certain pair of pinholes.

Defocused System and Wavefront Coding
We consider an optical system that suffers from defect of defocus in which a cubic phase mask has been included. The cubic phase mask has a peak-to-valley distance of α. The width of the exit pupil is *2R*. The generalized pupil function of an optical system with a defocus error is given by

$$\wp(x) = P(x)\, e^{i\, k\, W_{20}\, x^2 + \alpha\, x^3} \tag{7}$$

with $P(x)$ equals unity (if $|x| \leq R$) or zero (otherwise). We consider only a single pair of Young's pinholes placed at point x in the aberrated exit pupil and with spacing ε. In the absence of both defocus and wavefront coding, this pair would generate a sinusoidal fringe pattern of frequency $f = \varepsilon/\lambda\, z$. From Eq. (5) and Eq. (7), it follows that this infinitesimal element of the OTF is given by

$$H(f = \frac{\varepsilon}{\lambda\, z})\, dx = e^{i\, k\left[(3\alpha\,\varepsilon)x^2 + \left(\frac{4\pi}{\lambda}\, W_{20}\varepsilon\right)x + \frac{1}{4}\varepsilon^3\right]}\, dx \tag{8}$$

The contribution of all the phasors with this spacing is given by adding up all the infinitesimal elements in the area of overlap. The entire contributions to the real and imaginary parts of the OTF are plotted as a function of the distance x to the centre of the pupil in Fig. 10. Each curve represents one spatial frequency. The vector connecting one end of the curve, i.e. $H(-R)$, to the other, $H(R)$, represents the resultant OTF and its modulus is the MTF.

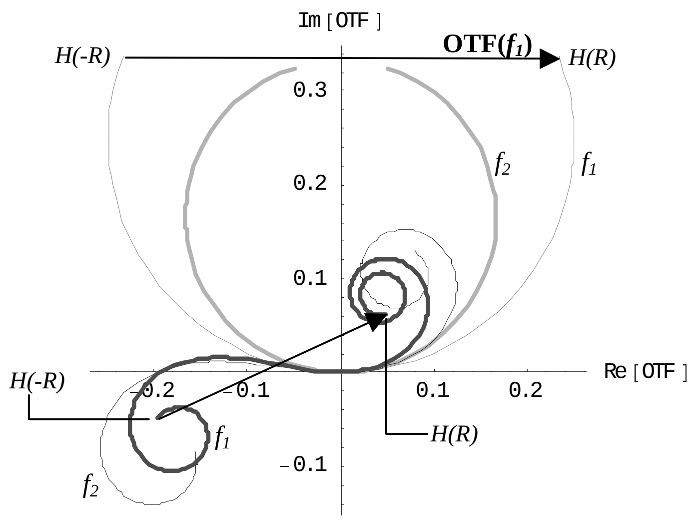

Figure 2. Parametric plot of the OTF as a function of the distance to the centre of the pupil. Each plot represents one spatial frequency (where $f_1 < f_2$). The circular curves correspond to a defocused system OTF. The spiral curves represent the OTF of a defocused system in which a cubic phase mask was placed, $\alpha = 5\lambda$ ($\lambda = 632.8\ nm$).

When the cubic element is removed, circular curves are obtained. As the separation between pinholes expands (moving to higher spatial frequencies) the radius of curvature of the plots decreases and eventually become circles. In this case, the final OTF will have only real part, with a magnitude equals the modulus of the vector parallel to the horizontal axes. Those frequencies in which $H(-R)=H(R)$, so that the gap closes and the curve is just completed, represent a null in the OTF and will not be transmitted by the system.

If the cubic phase mask is placed at the exit pupil, the quadratic factor in Eq. (8) will cause the previous defocused curves to curl (keeping their same length) generating spiral like curves, as shown in Fig. 10 for frequencies f_1 and f_2 (with $f_1 < f_2$). In this case, the new OTF will have both real and imaginary components as illustrated by the vector, however the distance between both extremes of the spiral $H(-R)$ and $H(R)$ will remain constant as the defocus term W_{20} is changed, see Fig. 11 and Fig. 12.

The peak-to-valley distance α in the cubic phase mask allows controlling the distance between the two extremes of the spiral. For relatively high values of α (α>20) it is possible to maintain the distance constant preventing the two ends to become together. Consequently, the OTF will have no zeros along the frequency spectrum, allowing digital deconvolution to restore the image.

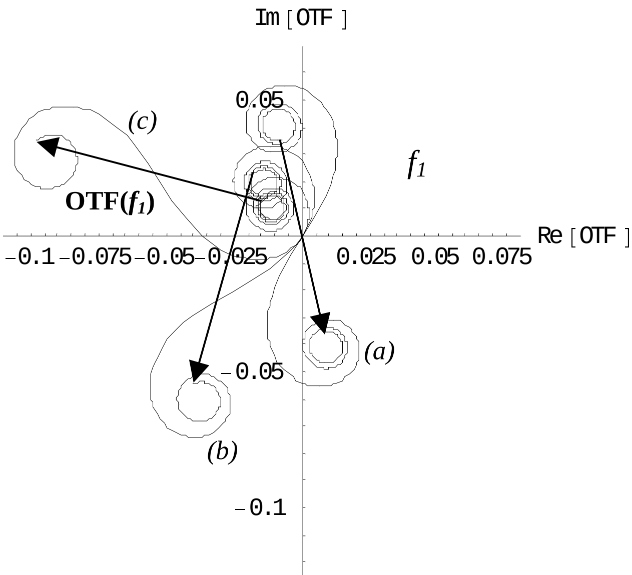

Fig. 11

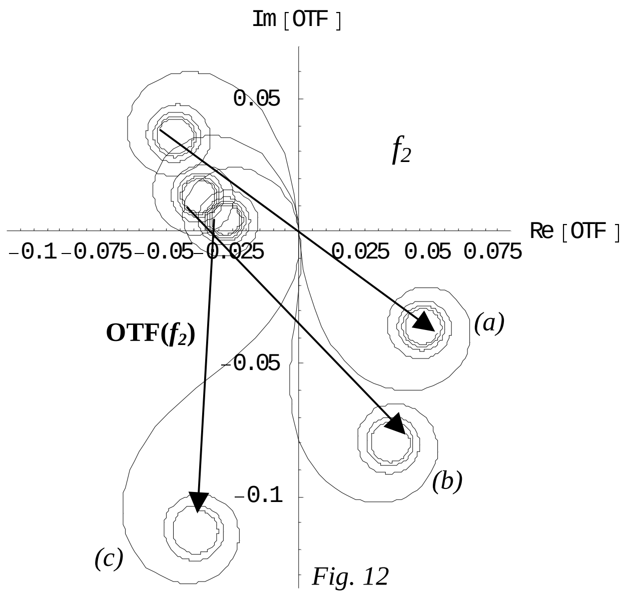

Fig. 12

Figure 11 and 12. OTFs for spatial frequency f_1 and f_2 ($f_1 < f_2$) when the defocus parameter is (a) $W_{20}=0$, (b) $W_{20}=1\lambda$ and (c) $W_{20}=2\lambda$. The modulus of the vector represent the MTF, it remains insensitive to defocus as W_{20} varies.

7. CONCLUSION

We have described the use of phase and amplitude filters for reduction in sensitivity to optical aberrations of defocus, spherical aberration, coma and astigmatism. Phase filters tend to enable better reductions in sensitivity to aberrations whilst retaining high optical throughput. The reduction in MTF for the aberrated optical systems that occurs with these phase filters will nevertheless generally reduce the SNR in the image although the lack of zeros means that, in general, deconvolution of images without loss of information, is still possible. The radially symmetric phase filters do not generally reduce the sensitivity to aberrations as efficiently as the cubic phase filter, but offer the advantage of low-cost manufacture.

8. ACKNOWLEDGEMENTS

This work was supported by QinetiQ, Malvern, United Kingdom.

REFERENCES

1. W. T. Welford, "Use of annular apertures to increase focal depth," J. Opt. Soc. Am. 50, 749-753 (1960)

2. M. Mino and Y. Okano, "Improvement in OTF of a defocused optical system through the use of shaded apertures," Appl. Opt. 10, 2219-2225 (1971)

3. M. J. Yzuel and F. Calvo, "A study of the possibility of image optimization by apodization filters in optical systems with residual aberrations," Opt. Acta 26 , 1397 1406 (1979)

4. J. Ojeda-Castaneda, L. R. Berriel-Valdos, and E. Montes, "Spatial filter for increasing the depth of focus," Opt. Lett., 10, 520-522, (1985)

5. J. Ojeda-Castaneda, P. Andres, and A. Diaz, "Annular apodizers for low sensitivity to defocus and to spherical aberration," Opt. Lett., 11, 487-489, (1986)

6. J. Ojeda-Castaneda, "Arbitrarily high focal depth with finite apertures," Opt. Lett., 13, 183-185, (1988)

7. G. Indebetouw and H. Bai, "Imaging with Fresnel zone pupil masks: extended depth of field," Appl. Opt., 23, 4299-4302, (1984)

8. J. Ojeda-Castaneda, P. Andres, A. Diaz, " Strehl ratio with low sensitivity to spherical aberration," J. Opt. Soc. Am. A, Vol. 5, 1233-1236, (1988)

9. C.J.R. Sheppard, "Synthesis of filters for specified axial proprieties," J. Mod. Opt. Vol. 43, 525-536, (1996)

10. D. Zalvidea, C. Colautti, E.E. Sicre, "Quality parameters analysis of optical imaging systems with enhanced focal depth using the Wigner distribution function," J. Opt. Soc. Am. A. 17, 867-873 (2000)

11. D. Zalvidea, E. E. Sicre, "Phase pupil functions for focal-depth enhancement derived from a Wigner distribution function," Appl. Opt. Vol. 37, 3623-3627 (1998)

12. S. Mezouari and A. R. Harvey, "Phase pupil functions for control defocus and spherical aberrations," submitted to Opt. Lett., (2002)

13. S. Mezouari and A. R. Harvey, "Primary aberrations alleviated with phase pupil filters," SPIE, *Novel Optical Systems Design and Optimization* V, Vol. 4768, 2002

14. Sucharita Sanyal, Ajay Ghosh, "High Tolerance to Spherical Aberrations and Defects of Focus with a Birefringent Lens," Appl. Opt. Vol. 41, 4611-4619, (2002)

15. H. Wang and F. Gan, "High focal depth with a pure-phase apodizer," Appl. Opt. 40, 5658-562 (2001)

16. E. R. Dowski, Jr., and W. T. Cathey, "Extended depth of field through wavefront coding," Appl. Opt. 34, 1859-1866 (1995)

17. J. van der Gracht, E. R. Dowski, Jr., W. T. Cathey, and J. P. Bowen, Aspheric optical elements for extended depth of field imaging, in Novel Optical Systems Design and Optimization, J. M. Sasian ed., Proc. SPIE 2537, 279 288 (1995)

18. S. S. Sherif, Ed. R. Dowski, W. T. Cathey, "A logarithmic phase filter to extend the depth of field of incoherent hybrid imaging systems," Proc. SPIE Vol. 4471, p.272-280 (2001)

19. S. Mezouari and A. R. Harvey, " Wavefront coding for aberration compensation in thermal imaging systems," Proc. SPIE Vol. 4442, p. 34-42, (2001)

20. A. T. Friberg, "Stationary-phase analysis of generalized axicons," J. Opt. Soc. Am. A, Vol. 13, 743-750, (1996)

21. M Born and E. Wolf, “Principles of Optics”, Cambirdge University Press, 1999.

22. J. Goodman, “Introduction of Fourier Optics”, Mc-Graw Hill, New York, 1996.